

Titanium Oxide (TiO₂) Nanoparticles Decorated Three-Dimensional Porous Nickel Foam Electrode for Non-Enzymatic Electrochemical Sensing of Glucose

M. B. Lakshmipriya¹, Tse-Wei Chen^{2,3}, Shen-Ming Chen^{2,*}, M. Chandrasekaran¹, G. N. K. Ramesh Babu^{1,*}, Ming-Chin Yu^{4,*}

¹ Electroplating Metal Finishing Technology Division, CSIR-Central Electrochemical Research Institute, Karaikudi-630003, Tamil Nadu, India.

² Electroanalysis and Bioelectrochemistry Lab, Department of Chemical Engineering and Biotechnology, National Taipei University of Technology, No.1, Section 3, Chung-Hsiao East Road, Taipei 106, Taiwan (R.O.C).

³ Research and Development Center for Smart Textile Technology, National Taipei University of Technology, Taipei 106, Taiwan, ROC.

⁴ Department of Surgery, Chang Gung Memorial Hospital, Taoyuan 333, Taiwan (R.O.C)

*E-mail: smchen78@ms15.hinet.net, mingchin2000@gmail.com, bapu2657@yahoo.com

Received: 18 February 2019 / Accepted: 22 April 2019 / Published: 30 June 2019

Three dimensional (3D) interconnected materials paid much attention in various field due to their significant electrical and catalytic properties. Here, 3D Ni-TiO₂ nanocomposite was prepared by wet impregnation method. The structure and morphology of the prepared 3D Ni-TiO₂ were characterized by scanning electron microscopy and electrochemical techniques, namely cyclic voltammetry and amperometry for non-enzymatic detection of glucose. The Ni-TiO₂ nanocomposite electrode showed excellent electrocatalytic activity towards the electro-oxidation of glucose molecule in an alkaline medium. The sensitivity was 844.85 $\mu\text{A mM}^{-1} \text{cm}^{-2}$ with selectivity towards the detection of glucose in the presence of interferences such as uric acid, ascorbic acid, and dopamine. The sensor was also used to determine the glucose in human blood serum samples.

Keywords: Ni-TiO₂ nanocomposite, Amperometry, Glucose sensor, Blood serum.

1. INTRODUCTION

Fast, quantitative, and reliable method for glucose monitoring is important in the field of biotechnology, clinical diagnostics, and food industry [1, 2]. Clark proposed the first enzymatic glucose biosensor in 1962 [3] that attracted significant attention in diabetes field. Conventional glucose sensors are based on an enzymatic reaction, in which glucose oxidase acted as a catalyst for the

oxidation of glucose to gluconolactone that showed high sensitivity and selectivity towards the glucose molecule. However, this sensor method shows some disadvantages including their high cost, poor stability and complicated enzyme immobilization procedure. Also, the intrinsic nature of enzymes is easily affected by temperature, pH, humidity and toxic chemicals [4, 5]. To solve these limitations, non-enzymatic glucose sensors has been proposed, which provided long term stability, rapid response and excellent sensitivity. Further, these electrochemical glucose sensor exhibits significant potential to selectively detect glucose molecule in blood samples, even in the presence of interfering molecules such as uric acid, ascorbic acid and dopamine [6]. Afterwards, it was discovered that the electro-oxidation of glucose depends extremely on the electrode materials, their crystalline orientation and the electrode surface. These have also been a determining factor for a non-enzymatic glucose sensor.

Different type of electrodes such as involving precious metals Pt, Au [7,8], transition metals Ni, Co, Cu [9-12], and their metal oxides NiO, CoO₂, CuO, MnO₂ [13-17], have been previously reported for non-enzymatic glucose detection. Additionally, because of the increased cost of the noble metals and easy poisoning of their surface, their importance in glucose sensing is restricted. Among these, Ni based electrode had been demonstrated as a promising material for non-enzymatic glucose sensors in alkaline medium [18]. It has effective electrocatalytic activity, low cost, most abundant, and highly electrically conductive property. In addition, different strategies have been reported to prepare nickel electrode material for electrochemical glucose sensing [19-22]. On the other hand, electrode dimension plays an important role for the detection of glucose. A three-dimensional permeation network of electrode fabrication provided an efficient electronic path way, effective mass transport and ion transport [23]. 3-D electrode material gives a large surface area and more reaction active sites than compared with 1-D and 2D structure electrode material. In recent days, Ni foam is widely exploited in energy efficient applications. Numerous nanomaterials including Co₃O₄/graphene, N-doped carbon nanotubes, polyaniline, nanoporous gold film and Pd nanoparticles had been effectively incorporated on 3D Ni foam and used for supercapacitor, Li-ion battery, zinc battery, H₂O₂ sensor, respectively [24–28]. Moreover, 3D porous Ni and FeS deposited Ni foam electrodes were also reported and used as a counter electrode in quantum dots solar cell application [29,30].

As metal nanoparticles have large surface area and intrinsic electrocatalytic properties, it was widely used as a modifier for glucose detection. Homogeneous distribution of nickel nanoparticles on the surface of straight multi-walled carbon nanotubes through in situ precipitation procedure and investigated for non-enzymatic glucose sensor [31]. TiO₂ nanotube arrays evenly modified by Ni-Cu nanoparticles were prepared by a potential step method for the application of glucose sensor [32]. Owing to the excellent conductivity, good chemical stability, large surface to volume ratio, high adsorption capacity and eco-friendliness, TiO₂ nanoparticles have been utilized as a nanoparticle support for non-enzymic glucose sensor. Recently, nickel associated with TiO₂ nanotubes and nanowires based composite materials are developed by several methods, for instance, Yu and co-workers [18] studied the anodization of Ti foil followed by pulse electrodeposition of Ni nanoparticles for the non-enzymatic glucose sensor. Guo and co-workers [33] fabricated Ti-TiO₂ nanowires on Ti foil followed by electrodeposition of CdS and Ni nanoparticles for high performance non-enzymatic glucose sensor. Longwei group [34] also prepared Ti/TiO₂ NTA/ Ni composite electrode via anodic oxidation for electrochemical glucose sensors. All these methods are time consuming processes.

Hence, in this article, the authors report a simple and rapid preparation of 3D Ni-TiO₂ nanocomposite electrode material and applied for the detection of glucose. 3D Ni-TiO₂ nanocomposite electrode showed excellent electrocatalytic activity towards glucose oxidation, which also exhibited greater selectivity to detect glucose molecules even in the presence of potential interfering species.

2. EXPERIMENTAL

2.1. Preparation of Ni-TiO₂ nanocomposite electrode

All chemicals were of analytical grade and used without further purification. The solutions were prepared using Millipore water. Ni-TiO₂ nanocomposite foam was prepared by wet impregnation method as follows: TiO₂ nanoparticle was prepared as described elsewhere [35] and was used in this work. 10 mg of TiO₂ nanoparticle precursor was suspended in 1 mL of 5 wt% Nafion with 10 mL water. This solution was ultrasonicated for 30 minutes. The Ni foam electrode area was 1x1cm². Before impregnation, it was pre-treated with acetone and ethanol for 2 minutes, then oxide layer was removed by dipping in 1 M HCl for 2 minutes. Later, the electrode was immersed in the ultrasonicated precursor solution with stirring for 15 minutes, then dried and used.

2.2. Characterization and electrochemical measurements

The surface morphology of Ni-TiO₂ nanocomposite foam and elemental composition were characterized using scanning electron microscope and energy dispersive X-ray spectrometer (SEM & EDAX: Hitachi, model 3000H) at an applied potential 15 kV. Electrochemical technique such as cyclic voltammetry and amperometry were used to investigate the redox behaviour of the modified three-dimensional electrodes and to perform glucose sensing experiments. Electrochemical measurements were carried out using Auto lab PGSTAT 30 with a three-electrode system including Ni-TiO₂ nanocomposite electrode as a working electrode, platinum plate as a counter electrode and Ag/AgCl as reference electrode.

3. RESULTS AND DISCUSSION

3.1 Materials characterization

Elemental distribution of Ni-TiO₂ nanocomposite was examined by EDAX (Fig. 1) which clearly indicates that TiO₂ nanoparticle was incorporated on three-dimensional bridging Ni foam. The nanocomposite is estimated to be 1.3 wt% of TiO₂ nanoparticle. Ni foam has advantages in terms of 3D open pore structure with high surface area, electronic conductivity and strong absorbing ability, suggesting it to be a good support for electrocatalytic material. Fig.2 revealed the surface morphology

of Ni and Ni-TiO₂ nanocomposite foam. TiO₂ nanoparticles absorbed by Ni foam and it mostly appear at the corner of the grid. Here, Ni showed pyramidal structure.

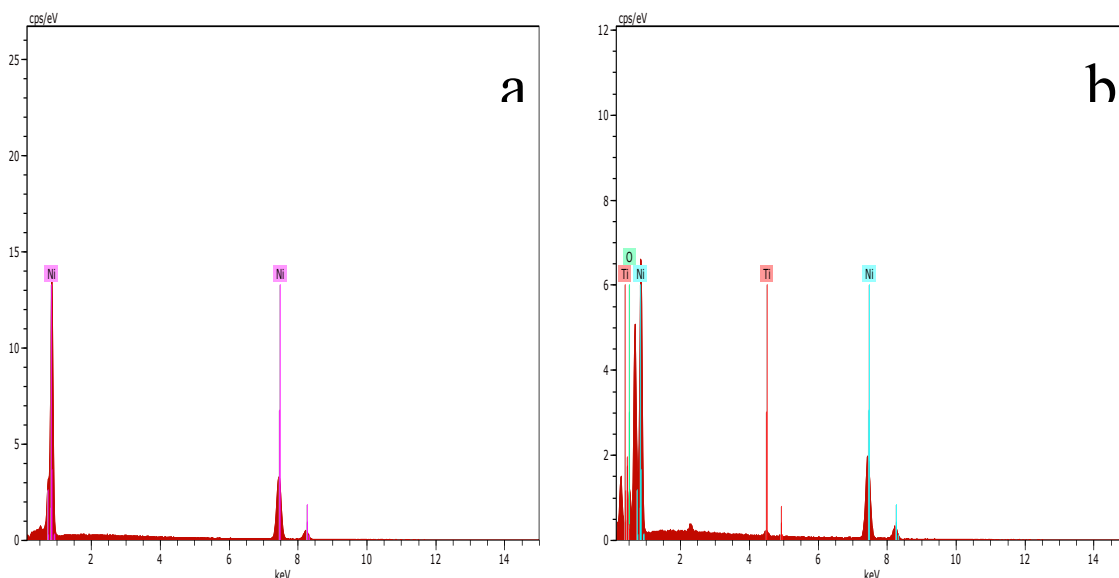


Figure 1. EDAX analysis of (a) bare Ni foam and (b) Ni-TiO₂ nanocomposite foam.

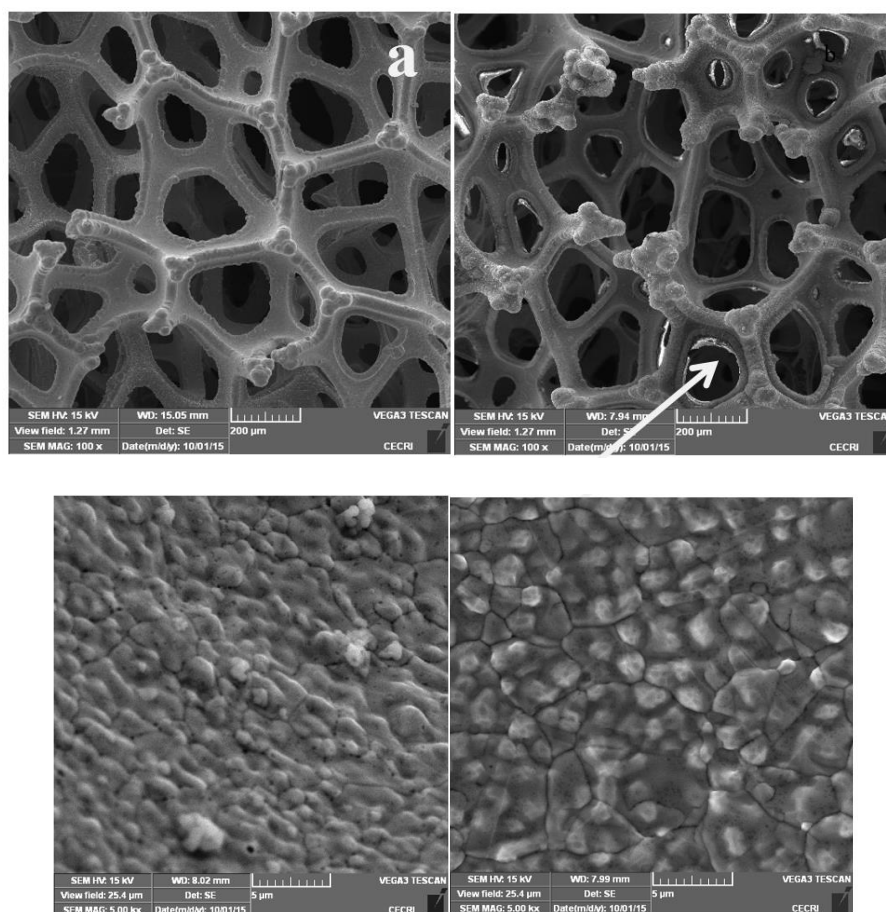


Figure 2. SEM image of (a) Ni foam at 100x. (b) Ni-TiO₂ nanocomposite foam at 100x (c) and (d) Ni-TiO₂ nanocomposite foam at 5K magnification.

3.2 Electrochemical performance of Ni-TiO₂ nanocomposite foam electrode

To investigate the electrochemical performance of the Ni-TiO₂ nanocomposite foam electrode, cyclic voltammetry was employed over a potential range from +0.1 to +0.75 V.

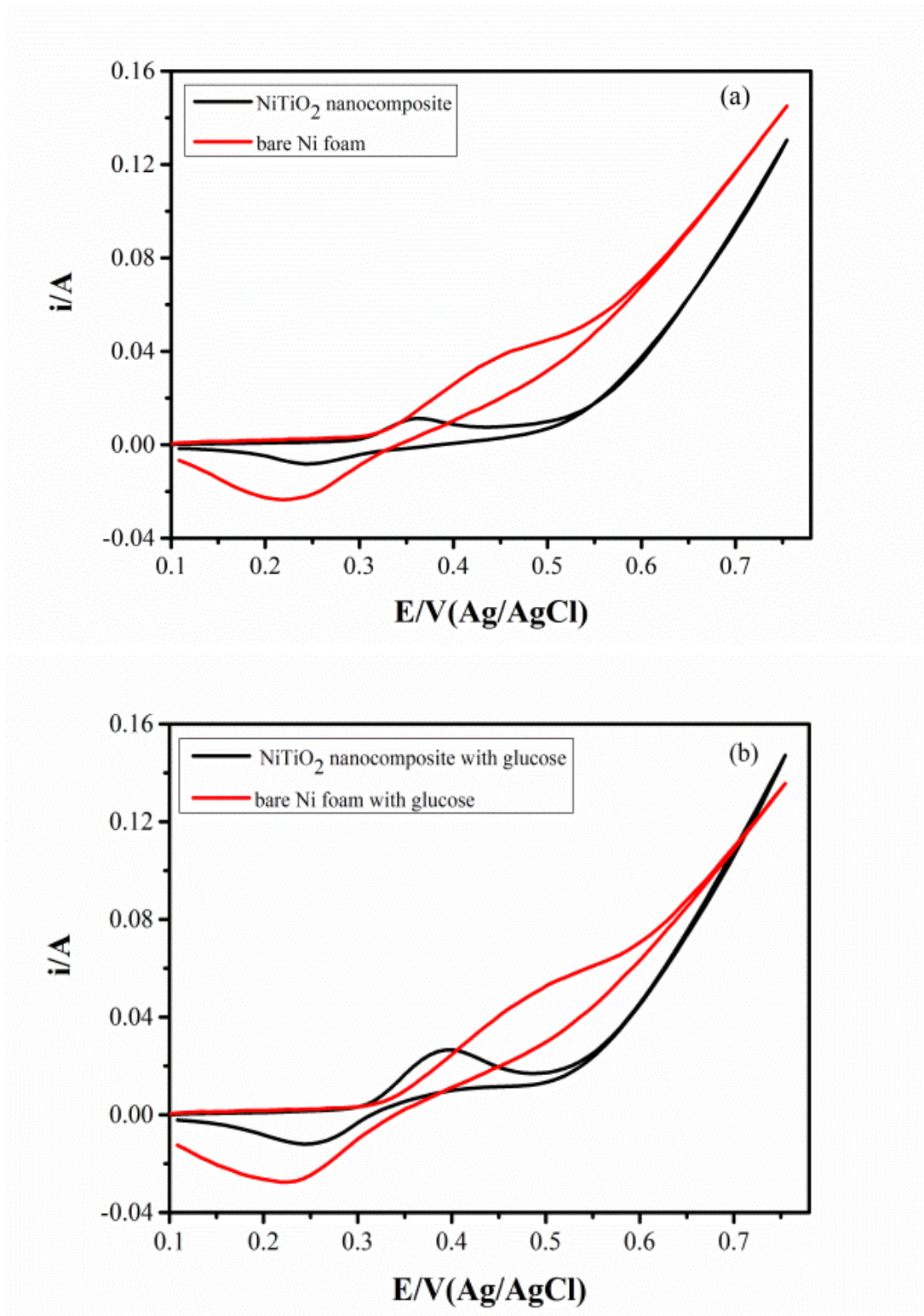


Figure 3. Cyclic voltammograms for Ni-TiO₂ nanocomposite and bare Ni foam electrode response (a) without (b) with glucose in 0.1M NaOH solution at 200mVs⁻¹.

Table 1. Cyclic voltammetry parameters for bare Ni foam and modified Ni-TiO₂ nanocomposite foam electrode without and with glucose.

| Electrode | Without glucose | | With glucose | |
|--|-----------------|---------------------------------|--------------|---------------------------------|
| | E_{pa} | I_{pa} | E_{pa} | I_{pa} |
| Bare Ni foam electrode | 0.436V | $5.307 \times 10^{-3} \text{A}$ | 0.478V | $5.830 \times 10^{-3} \text{A}$ |
| Ni-TiO ₂ nanocomposite foam electrode | 0.360V | $6.766 \times 10^{-3} \text{A}$ | 0.394V | $16.25 \times 10^{-3} \text{A}$ |

As depicted in Fig. 3, the cyclic voltammograms of the bare Ni foam electrode and NiTiO₂ nanocomposite foam electrode (a) without and (b) with glucose in 0.1 M NaOH solution at a scan rate 200 mVs⁻¹ (vs. Ag/AgCl). A pair of well-defined redox peaks with anodic peak potential (E_{pa}) at 0.360 V corresponding to the cathodic peak potential (E_{pc}) at 0.23 V were observed on Ni-TiO₂ nanocomposite foam electrode. The current and potential for bare Ni foam and modified Ni-TiO₂ nanocomposite foam electrode were summarized in Table 1. As seen in Fig. 3(a), anodic peak potential of bare occurred at 0.436 V, later it is shifted into 0.360 V while incorporating the TiO₂ nanoparticles on Ni foam. This is due to the n-type characteristics of TiO₂ nanoparticle having high specific surface area and well aligned nanostructure. Also, the observed Ni-TiO₂ nanocomposite anodic peak current (i_{pa}) $5.830 \times 10^{-3} \text{A}$ was higher than the bare Ni foam (i_{pa}) $5.307 \times 10^{-3} \text{A}$ electrode. These results indicate that TiO₂ nanoparticle enhances the electrocatalytic activity of Ni-TiO₂ nanocomposite. Under the alkaline conditions, Ni (0) was associated with OH⁻ ions and generated Ni (II) ions. It was further proceeded by the oxidation of Ni(II)/ Ni(III) redox couple as revealed in Fig. 3(a) at $E_{pa} = 0.360 \text{V}$ vs. (Ag/AgCl) and described in Eq (1) and (2).

The electrochemical reactions of the Ni(II)/ Ni(III) peaks followed [29];

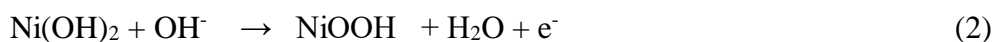


Fig. 3(b) revealed the electrocatalytic activity of the Ni-TiO₂ nanocomposite electrode towards glucose oxidation. The as-prepared Ni-TiO₂ nanocomposite structure was mechanically and chemically stable. It has fine groove like skeleton with high porosity which helped to increase the active surface area and allowed rapid glucose transport with large surface area of TiO₂ nanoparticle to increase the number of active sites of the Ni (III) formation. When the glucose solution was added, remarkable increase of the oxidation current was observed. This is attributed to the electro-oxidation of glucose to gluconolactone by the as-formed Ni (III), as shown in Eq (3).



Once the Ni(III) species was produced by the electrode, it rapidly oxidizes glucose at the anodic potential (E_{pa}) sacrificing Ni(III) and producing reduced Ni(II) species at the cathodic sweep potential (E_{pc}), which in turn it was further oxidized under the anodic voltage. In addition, the electrocatalytic activity of Ni-TiO₂ nanocomposite toward various concentration of glucose was examined by cyclic voltammetry in 0.1 M NaOH solution at a scan rate 200 mVs⁻¹. Upon increment in glucose concentration, the significant enhancement was noticed in anodic peak currents associated with the positive shifts in anodic peak potential. Furthermore, cathodic peak current decreased with an increase in the concentration of glucose. It indicates the electrooxidation of glucose at Ni-TiO₂ nanocomposite foam electrode was a quasi-reversible electrochemical process [36, 37].

3.3 Application of the 3D Ni-TiO₂ nanocomposite electrode in non-enzymatic glucose sensing

The simple fabrication procedure makes the as-prepared electrode an effective platform for the amperometric determination of glucose. Importantly, the smaller background current with lower noise observed at an applied optimized potential of 0.45 V and selected for glucose detection. Fig. 5(a) shows the amperometric response of the 3D Ni-TiO₂ nanocomposite electrode towards the successive stepwise addition of glucose in 0.1 M NaOH solution and homogeneously stirred condition.

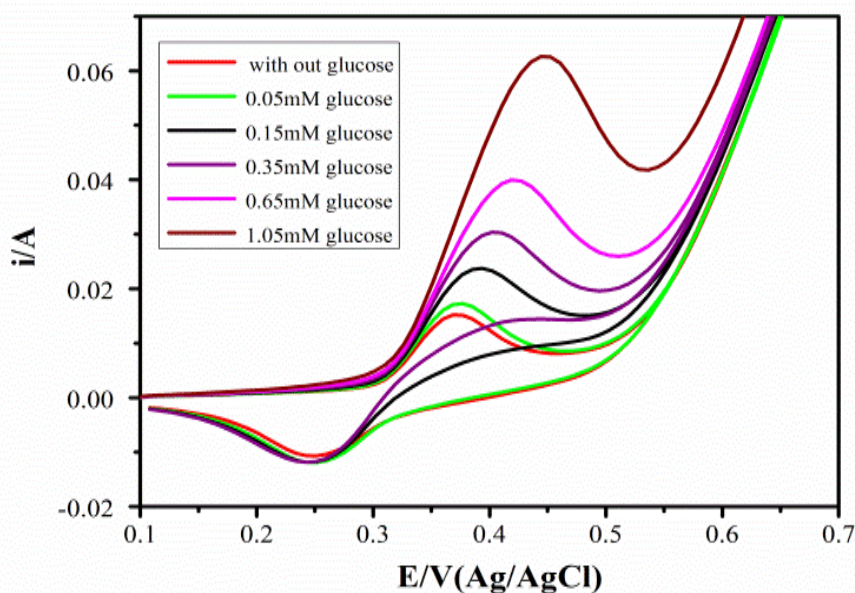


Figure 4. Cyclic voltammograms of the Ni-TiO₂ nanocomposite electrode in the presence of various concentration of glucose (0.05, 0.15, 0.35, 0.65, 1.05mM) in 0.1M NaOH solution scan rate at 200 mv s⁻¹.

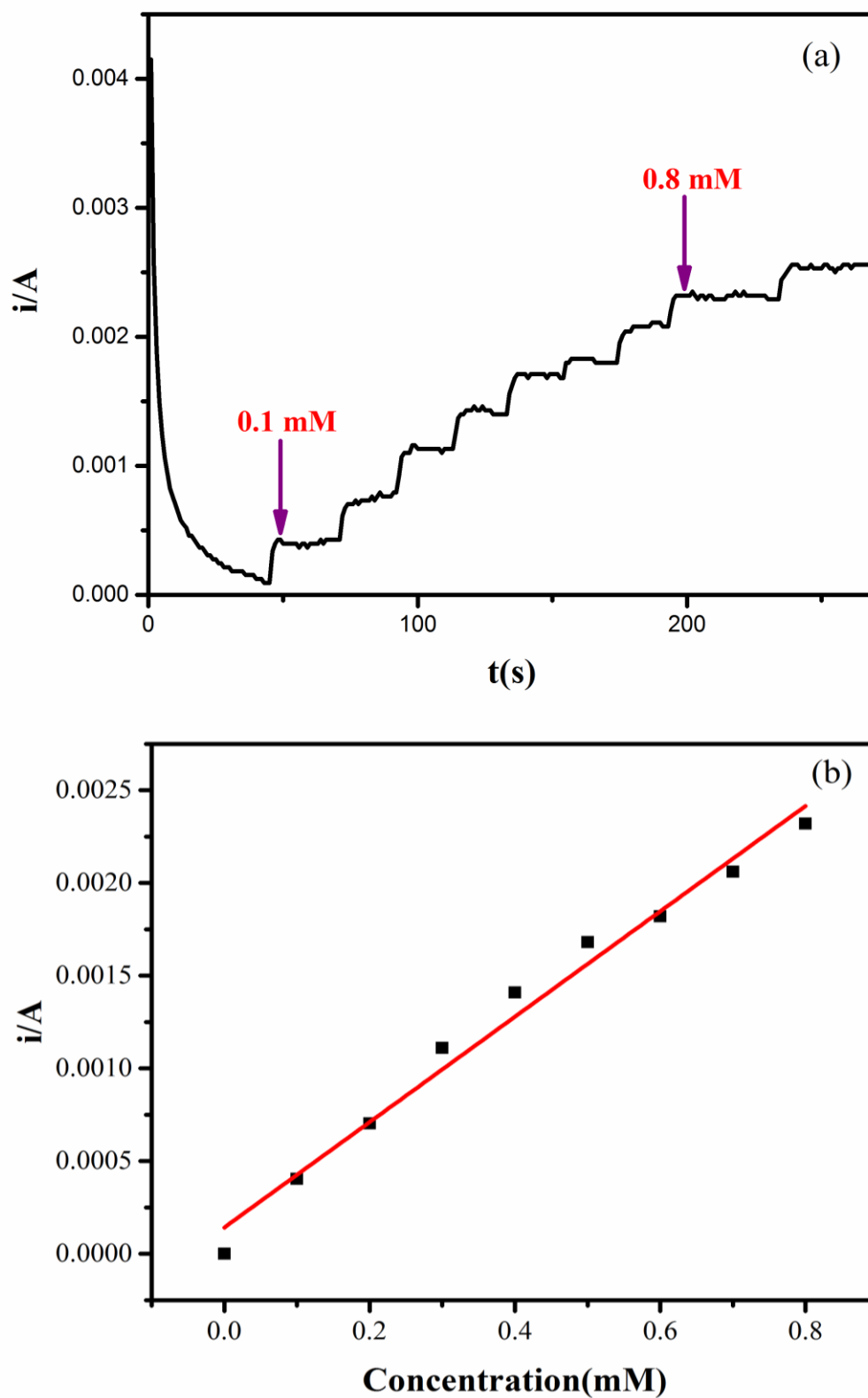


Figure 5. (a) Amperometric response of the Ni-TiO₂ nanocomposite foam electrode with successive addition of glucose at 0.45V in 0.1M NaOH solution. (b) The corresponding calibration curve.

A steady state current was achieved at less than seconds and a substantial steep increase in current responses was obtained after each addition of 0.1 mM glucose solution. It was indicating that the 3D Ni-TiO₂ electrode exhibits sensitive and rapid response characteristics. This might be due to the fact that 3D interconnected porous structure provides low resistance and promote electron transfer to reduce the response time. The corresponding calibration curve presented in Fig. 5(b) shows linear over a concentration range from 0.1 to 0.8 mM of glucose with a correlation coefficient was 0.9937 and limit of detection of 66 μM at a signal to noise ratio of 3. The sensitivity of the Ni-TiO₂ nanocomposite electrode was calculated to be 844.85 μA mM⁻¹ cm². This remarkable sensitivity is attributed to its porous structure that enhances electrical and catalytic properties. Ni-TiO₂ nanocomposite electrode showed higher electrocatalytic activity toward non-enzymatic glucose sensing in comparison with the earlier reports as given in Table 2. [38-42]

Table 2. Comparison of Ni-TiO₂ nanocomposite foam electrode with other reported modified electrode for glucose sensors.

| Electrode | Electrode modifier | Method | Sensitivity μA mM ⁻¹ cm ² | Linear range | Reference |
|-----------|-------------------------------------|-------------|--|--------------|--------------|
| GCE | Ni(OH) ₂ NP/Chitosan | Amperometry | 72 | 0.5-10 mM | 38 |
| GCE | Ni(OH) ₂ /Au | Amperometry | 371.2 | 0.005-2.2mM | 39 |
| GCE | NiO@ PPy/Au | Amperometry | 802.9 | 0.5-1.7mM | 40 |
| GCE | Cu-NiO | Amperometry | 171.8 | 0.5μM-5mM | 41 |
| Ni foam | NiO/CeO ₂ | Amperometry | 154.4 | 1-2900 μM | 42 |
| Ni foam | NiTiO ₂ nanocomposite | Amperometry | 844.85 | 0.05-0.8mM | Present work |

3.4 Interference test

While analyzing glucose in blood serum samples, uric acid (UA), dopamine (DA), and ascorbic acid (AA) may interfere with the detection of glucose. The normal physiological level of glucose in blood serum is around 3–7 mM which is much higher when compared to the concentration of interfering species. Thus, the interference test was carried out with a 0.1 mM and 0.5 mM of glucose and fixed concentration of 0.1 mM for interfering species and followed the experimental details as in section 3.3. As shown in Fig. 6, the current response was negligible for UA, DA and AA after adding 0.5 mM of glucose. It indicates the Ni-TiO₂ nanocomposite electrode has good selectivity towards the detection of glucose even in presence of other interferences.

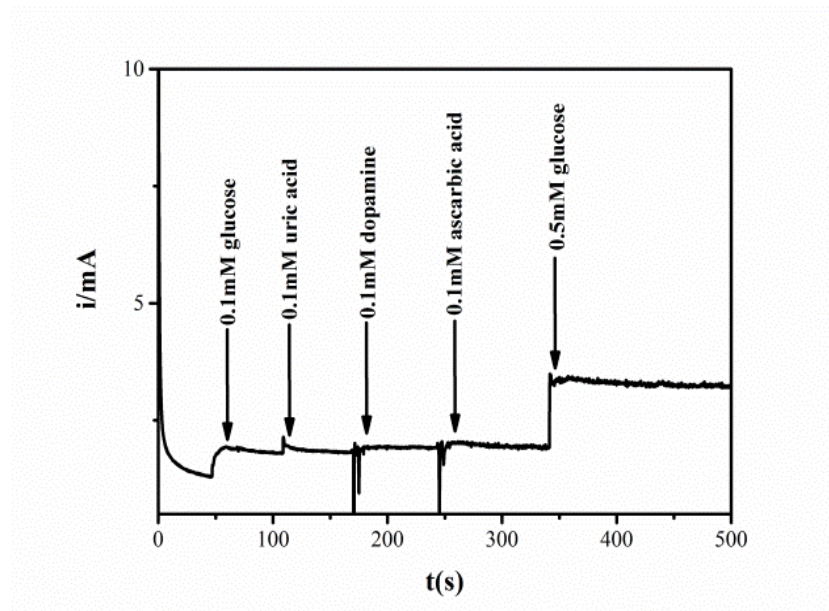


Figure 6. Interference test of the Ni-TiO₂ nanocomposite foam upon the successive injection of glucose and possible interfering species at 0.45V in 0.1M NaOH solution.

3.5 Real sample analysis

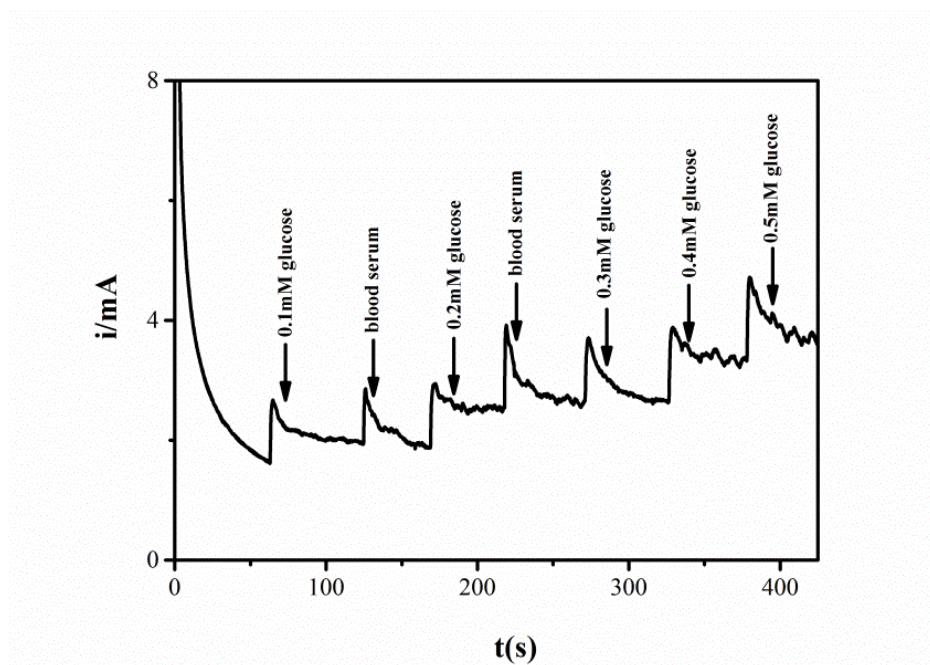


Figure 7. Amperometric current response of the Ni-TiO₂ nanocomposite foam in the presence of various concentration of glucose followed by blood serum samples at 0.45V in 0.1M NaOH solution.

To evaluate the ability of the sensor for routine analysis, determination of glucose in human blood serum samples was also performed on the 3D Ni-TiO₂ nanocomposite electrode. Fig. 7 showed

the amperometric response of Ni-TiO₂ nanocomposite electrode toward 0.1 and 0.2 mM of standard glucose followed by the alternative addition of human blood serum sample. 200 μ L of blood serum was added into 20 mL of 0.1 M NaOH electrolyte solution at 0.45 V and the current response was successfully recorded. The recovery studies were presented in Table 3 which indicated that the proposed sensor has a good sensing potential under the practical application.

Table 3. Glucose detection in blood serum samples

| Sample | Glucose added (mM) | Glucose found (mM) | Recovery |
|----------|--------------------|--------------------|----------|
| Sample-1 | 0.055 | 0.0525 | 95.5% |
| Sample-2 | 0.055 | 0.0579 | 105.2% |

4. CONCLUSIONS

In this study, the simple fabrication method of 3D Ni-TiO₂ nanocomposite foam designed for the electrochemical sensing of glucose was demonstrated. The SEM analysis showed that TiO₂ nanoparticles decorated onto the Ni foam surface. It exhibits high sensitivity 844.85 μ AmM⁻¹ cm⁻² also revealed excellent selectivity towards the detection of glucose. The use of this glucose sensor in human blood serum has also been tested successfully.

ACKNOWLEDGEMENT

The authors gratefully acknowledge the financial support of the National Taipei University of Technology and Chang Gung Memorial Hospital Joint Research Program (NTUT-CGMH-108-05) and CORPG1I0011. The authors thank the Director, CSIR-CECRI for his kind permission to publish the paper and the financial support by MULTIFUN project.

References

1. P. Yang, X. Tong, G. Wang, Z. Gao, X. Guo and Y. Qin, *ACS Appl. Mater. Interfaces.*, 7 (2015) 4772.
2. R. Prasad, N. Gorjizadeh, R. Rajarao, V. Sahajwallab and B.R. Bhat, *RSC Adv.*, 5 (2015) 44792.
3. Clark, L. C, Lyons, C. *Ann. NY Acad. Sci.*, 102 (1962) 29.
4. C. Guo, Y. Wang, Y. Zhao and C. Xu, *Anal. Methods.*, 5 (2013) 1644.
5. C. Guo, X. Zhang, H. Huo, C. Xu and X. Han, *Analyst*, 138 (2013) 6727.
6. W. Lv, F.M. Jin, Q. Guo, Q.H. Yang, F. Kang, *Electrochim. Acta*, 73 (2012) 129.
7. A.M.V. Mohan, K.K. Aswini, A.M. Starvin and V. M. Biju, *Anal. Methods.*, 5 (2013) 1764.
8. G.X. Zhong, W.X. Zhang, Y.M. Sun, Y.Q. Wei, Y. Lei, H.P. Peng, A.L. Liu, Y.Z. Chen, X.H. Lin, *Sens. Actuators B Chem*, 212 (2015) 72.

9. G. Yang, E. Liu, N.W. Khun, S.P. Jiang, *J. Electroanal Chem*, 627 (2009) 51.
10. K.M. Hassan, G.M. Elhaddad, M.A. Azzem, *J. Electroanal Chem*, 728 (2014) 123.
11. S. Premlatha, P.Sivasakthi and G. N. K. Ramesh Babu, *RSC Adv.*, 5 (2015) 74374.
12. S. Hussain, K. Akbar, D. Vikraman, D.C. Choi, S.J. Kim, K.S. An, S. Jung and J. Jung, *New J. Chem.*, 39 (2015) 7481.
13. B. Yuan, C. Xu, D. Deng, Y. Xing, L. Liu, H. Pang, D. Zhang, *Electrochim. Acta*, 88 (2013) 708.
14. A.M. Ghonim, B.E.E. Anadouli, M.M. Saleh, *Electrochim. Acta*, 114 (2013) 713.
15. X. Wang, X. Dong, Y. Wen, C. Li, Q. Xiong and P. Chen, *Chem. Commun.*, 48 (2012) 6490.
16. M.F. Wang, Q.A. Huang, X.Z. Li and Y. Wei, *Anal. Methods*, 4 (2012) 3174.
17. J. Chen, W.D. Zhang, J.S. Ye, *Electrochem Commun.*, 10 (2008) 1268.
18. S. Yu, X. Peng, G. Cao, M. Zhou, L. Qiao, J. Yao, H. He, *Electrochim. Acta*, 76 (2012) 512.
19. Z. Cui, H. Yin, Q. Nie, D. Qin, W. Wu, X. He, *J Electroanal Chem*, 757 (2015) 51.
20. H. Tian, M. Jia, M. Zhang, J. Hu, *Electrochim. Acta*, 96 (2013) 285.
21. P. Subramanian, J.N. Jonsson, A. Lesniewski, Q. Wang, M. Li, R. Boukherrou and S. Szunerits, *J. Mater. Chem. A*, 2 (2014) 5525.
22. Amgad S. Danial, M.M. Saleh, S.A. Salih, M.I. Awad, *J Power Sources*, 293 (2015) 101.
23. D.R. Rolison, J.W. Long, J.C. Lytle, A.E. Fischer, C.P. Rhodes, T.M. McEvoy, M.E. Bourga and A. M. Lubers, *Chem. Soc.Rev*, 38 (2009) 226.
24. J. Huang, J. Zhu, K.Cheng, Y. Xu, D. Cao, G. Wang, *Electrochim. Acta*, 75 (2012) 273.
25. S. Khamlich, T. Mokrani, M.S. Dhlamini, B.M. Mothudi, M. Maaza, *Energy Procedia*, 88 (2016) 614.
26. J. Wu, W.J. Yin, W.W. Liu, P. Guo, G. Liu, X. Liu, D. Geng, W.M. Lau, H. Liu and L.M. Liu, *J. Mater. Chem. A*, 4 (2016) 10940.
27. Y. Xia, D. Zhu, S. Si, D. Li, S. Wu, *J Power Sources*, 283 (2015) 125.
28. X.Ke, Y. Xu, C. Yu, J. Zhao, G. Cui, D. Higgins, Z. Chen, Q. Li, H. Xu and G. Wu, *J. Mater. Chem. A*, 2 (2014) 16474.
29. W. Lu, X. Qin, A.M. Asiri, A.O. Al-Youbi and X. Sun, *Analyst*, 138 (2013) 417.
30. H. Geng, L. Zhu, W. Li, H. Liu, L. Quan, F. Xi, X. Su, *J Power Sources*, 281 (2015) 204.
31. H. Nie, Z. Yao, X. Zhou, Z. Yang, S. Huang, *Biosens Bioelectron*, 30 (2011) 28.
32. X. Li, J. Yao, F. Liu, H. He, M. Zhou, N. Mao, P. Xiao, Y. Zhang, *Sens Actuators B Chem*, 181 (2013) 501.
33. C. Guo, H. Huo, X. Han, C. Xu, and H. Li, *Anal.Chem*, 86 (2014) 876.
34. C. Wang, L. Yin, L. Zhang, and R. Gao, *J. Phys. Chem. C*, 114 (2010) 4408.
35. A.M.K. Kirubakaran, M. Selvaraj, K. Maruthan, D. Jeyakumar, *J. Coat. Technol. Res*, 9 (2012) 163.
36. A.J. Bard, L.R. Faulkner, *Electrochemical Methods: Fundamentals and Applications*, 2001, Second edition John Wiley & Sons, Inc., New York.
37. P.Sivasakthi, G.N.K. Ramesh Babu, M. Chandrasekaran, *Mater. Sci. Eng. C*, 58 (2016) 789.
38. A. Ciszewski, I. Stepniak, *Electrochim Acta*, 111 (2013) 185.
39. J. Chen, J. Zheng, *J Electroanal Chem*, 749 (2015) 83.
40. J. Chen, Q. Sheng and J. Zheng, *RSC Adv.*, 5 (2015) 105372.
41. X. Zhang, A. Gu, G. Wang, Y. Huang, H. Jia and B. Fang *Analyst*, 136 (2011) 5175.
42. J. Cui, J. Luo, B. Peng, X. Zhang, Y. Zhang, Y. Wang, Y. Qin, H. Zheng, X. Shu, and Y. Wu, *Nanoscale*, 8 (2016) 770.